SciForschen
Open HUB for Scientific Research

ISSN 2575-0305

Journal of Molecular Medicine and Clinical Applications

Research Article | Volume: 2.1 | Open Access

Nanopore Transducer Engineering and Design

Stephen Winters-Hilt[1,2,3]*

[1]*Biology Department, Connecticut College, Connecticut, USA*
[2]*Computer Science Department, Connecticut College, Connecticut, USA*
[3]*Meta Logos Inc., Connecticut, USA*

***Corresponding author:** Stephen Winters-Hilt, 270 Mohegan Ave, New London, Connecticut 06320, USA, Tel: +1-985-789-2258; **E-mail:** swinters@conncoll.edu

Received date: 23 Mar 2017; **Accepted date:** 19 Apr 2017; **Published date:** 26 Apr 2017.

Citation: Winters-Hilt S (2017) Nanopore Transducer Engineering and Design. J Mol Med Clin Appl 2(1): doi http://dx.doi.org/10.16966/2575-0305.108

Abstract

The nanopore transduction detector (NTD) platform comprises a single nanometer scale channel and an engineered, or selected, channel blockading molecule. The channel current blockade molecules are engineered to provide distinctive stationary channel blockade statistics, with changes in the channel blockade stationary statistics upon transducer binding to interaction target. In single-molecule characterization the NTD functions like a 'nanoscope', e.g., a device that can observe the states of a single molecule or molecular complex. With the NTD apparatus the observation is not in the optical realm, like with the microscope, but in the molecular-state classification realm. NTD, thus, provides a new technology for characterization of single molecules and transient complexes in a variety of biosensing, assaying, and single-molecule conformation/binding studies. The nanopore detection method uses the stochastic carrier wave signal processing methods, developed and described in prior work that comprises machine learning methods for pattern recognition that can be implemented on a distributed network of computers for real-time experimental feedback and sampling control. Nucleic acid based transducers are described that are channel modulators whether bound or unbound. The nucleic acid transducer blockade modes are found to be dominated by the physical rigid-body (toggle) modes and internal twist modes of the nucleic acid. A proliferation of modes beyond toggling and twisting is not seen, even under a variety of high strain conditions on the channel-captured transducer. Nucleic acid and antibody based transducers can be used for biosensing, assaying, and therapeutic applications. The therapeutic transducers can offer targeted delivery to particular tissue type, or provide more complex targeted binding via chelation.

Keywords: Nanopore detector; Nanopore transduction detection

Abbreviations: NTD: Nanopore Transduction Detection

Introduction

The nanopore transduction detector (NTD) platform [1,2] includes a single nanometer scale channel and an engineered, or selected, channel blockading molecule. The channel blockading molecule is engineered to provide a current modulating blockade in the detector channel when drawn into the channel, and held, by electrophoretic means. The channel has inner diameter at the scale of that molecule. For most biomolecular analysis implementations this leads to a choice of channel that has inner diameter in the range 0.1-10 nanometers to encompass small and large biomolecules, where the inner diameter is 1.5 nm in the alpha-hemolysin protein based channel used in the results that follow. Given the channel's size it is referred to as a nanopore in what follows. In efforts by others 'nanopore' is sometimes used to describe large 100-1000 nm range channels, which are here referred to here as micropores.

In order to have a capture state in the channel with a single molecule, a true nanopore is needed, and to establish a coherent capture-signal exhibiting non-trivial stationary signal statistics the nanopores limiting inner diameter typically needs to be sized at approximately 1.5nm for duplex DNA channel modulators (precisely what is found for the alpha-hemolysin channel in Figure 1). The modulating-blockader is captured at the channel for the time-interval of interest by electrophoretic means, which is established by the applied potential that also establishes the observed current flow through the nanopore.

The NTD molecule providing the channel blockade has a second functionality, typically to specifically bind to some target of interest, with blockade modulation discernibly different according to binding state [2-4] (such as with the Biotin-Streptavidin example in Figure 2, or with DNA annealing). NTD modulators are, thus, engineered to be bifunctional: one end is meant to be captured and modulate the channel current, while the other, extra-channel-exposed end, is engineered to have different states according to the event detection. Examples include extra-channel ends linked to binding moieties such as antibodies, antibody fragments, Aptamers, or nucleic acid (for annealing-to-complement nucleic acid detection). Examples also include 'reporter transducer' molecules (for signal amplification) with cleaved/uncleaved extra-channel-exposed ends, with cleavage by, for example, UV or enzymatic means [1]. By using signal processing with pattern recognition to manage the channel current blockade modulations, and thereby track the molecular states engineered into the transducer molecules, a biosensor or assayer is enabled.

In Figure 2 we see that Bt-8gc transducer produces a fixed-level blockade when bound to streptavidin. In an effort to 'awaken' the captured bound transducer into a modulatory mode, as well as to examine the impact of chaotrope in general, 2M urea is introduced at 6000s, with steady increase in urea concentration to 3.5M by 8,000s. No change to the modulatory signal for the bound transducers was observed, and no degradation in the NTD performance was seen. Further exploration of the NTD platform in the presence of more extreme chaotrope was done with Bt-8gc transducer examined in urea concentrations up to 5M (Figure 3) [5]. As Figure 3 reveals, the transducer has a racemic mixture of two discernibly different conformations, or isomers, when chaotrope is at high concentration.

In previous work it was shown that the presence of a specific five base length nucleic acid could be ascertained using NTD [3], and that an eight base sequence of DNA could be ascertained with very high specificity

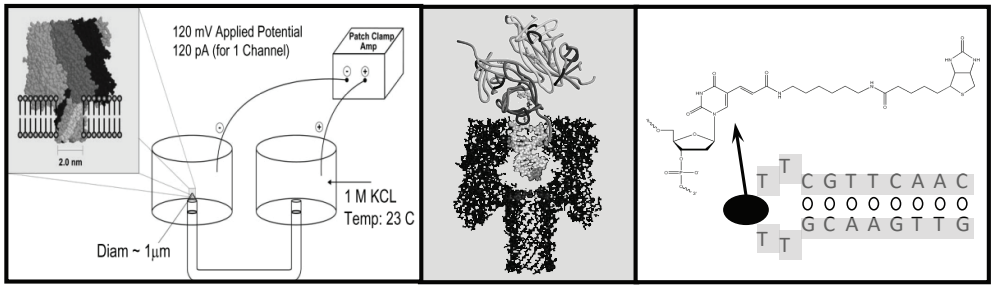

Figure 1: Schematic diagram of the Nanopore Transduction Detector**:** Reprinted with permission of Winters-Hilt S [2]. Left: the nanopore detector consists of a single pore in a lipid bilayer which is created by the oligomerization of the staphylococcal alpha-hemolysin toxin in the left chamber, and a patch clamp amplifier capable of measuring pico Ampere channel currents located in the upper right-hand corner. Center: shows a biotinylated DNA hairpin molecule captured in the channel's cis-vestibule, with streptavidin bound to the biotin linkage that is attached to the loop of the DNA hairpin. Right: shows the biotinylated DNA hairpin molecule (Bt-8gc).

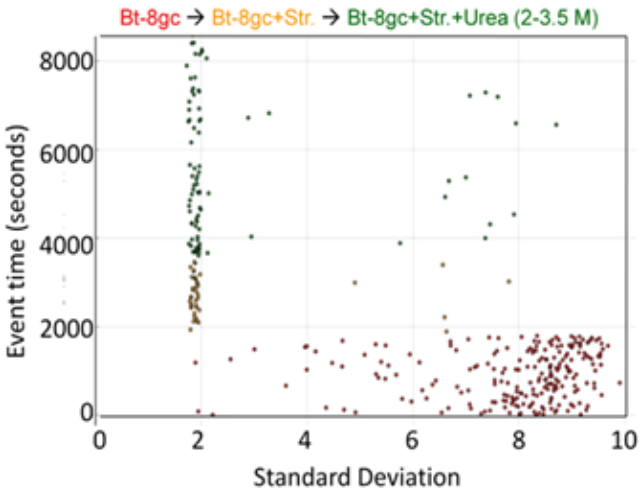

Figure 2: Biotin-streptavidin binding studies where bound transducer has a fixed-level blockade: Observations of individual blockade events are shown in terms of their blockade standard deviation (x-axis) and labeled by their observation time (y-axis) Reprinted with permission of Winters-Hilt S [2]. The standard deviation provides a good discriminatory parameter in this instance since the transducer molecules are engineered to not provide a fixed-level blockade (when unbound at least), thus have a notably higher standard deviation than typical noise or contaminant signals. At T=0 seconds, 1.0 µM Bt-8gc is introduced and event tracking is shown on the horizontal axis via the individual blockade standard deviation values about their means. At T=2000 seconds, 1.0 µM Streptavidin is introduced. Immediately thereafter, there is a shift in blockade signal classes observed to a fixed-level blockade signal, as can be visually discerned. The new signal class is hypothesized to be due to (Streptavidin)-(Bt-8gc) bound-complex captures.

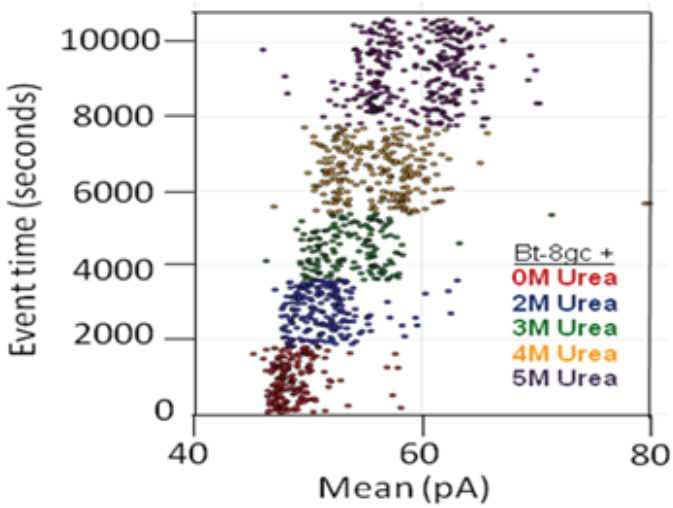

Figure 3: Bt-8gc transducer blockade signals in the presence of high urea concentrations: Reprinted with permission of Winters-Hilt S [5]. Sufficiently strong Urea concentration (5M) results in racemization of the two loop capture-variants, while weaker urea (<2M) does not. The results show Bt-8gc measurements at 30 minute intervals (1800 s on vertical axis) with urea concentration 0, 2, and 3M, 45 minutes at 4M, and 60 minutes at 5 M, with signal blockade mean on the x-axis. The results are consistent with the two-state loop hypothesis, and consistent with the observations [2] (see Figure 1),that were not due to high urea content but due to high strain due to mass and charge effects upon binding.

which could be further enhanced with the introduction of urea as a chaotrope. Using chaotrope when working with collective binding events (such as DNA annealing) allows clearer separation of annealed and un-annealed states [2].

Eight and nine base-pair DNA hairpins have been used as channel modulators [2], where the modulator has had a covalently attached binding moiety (biotin or linked antibody) that was tracked as to its binding state according to the channel modulation exhibited by their channel-captured DNA hairpin ends (see Figure 1 and other figures from [1] for the biotin-streptavidin binding study). Further developments along these lines without using a linker arrangement, where a more commoditized immuno-PCR tagging methodology is used, has led to the DNA 'Y-transducer' platform (for aptamer-based biosensing see background section, for monoclonal antibody biosensing [4,6], see background section). The Y-transducer was used in experiments showing DNA-DNA annealing on 5-9 base nucleic acids, and in transducing DNA-protein binding events: HIV integrase and TATA-binding protein (TBP) [7,8]. A limitation in all of these efforts was that the critical length of duplex nucleic acid needed for modulation, even in an unbound state, ranged from 8 to 10 base-pairs for the alpha-hemolysin nanopore platform that was being used. (Reasons for using the alpha-hemolysin platform have been described elsewhere [1], and won't be discussed further here.) The short duplex lengths meant that the reporter molecule could only be observed for seconds or minutes before melting, forcing the NTD to operate in a rapid-sampling 'ensemble' detection mode on the transducer/reporter molecules [9], and less in the single-molecule event-tracking mode that might otherwise be optimal for some applications.

Two problems with the NTD approach are, thus, revealed in the Bt-8gc transducer study: (1) fixed-level blockade by the bound transducer; and (2) isomer splitting on the transducer itself under high strain conditions (such as high chaotrope). In this paper we show how to eliminate both of these problems**.** Further introductory details are thus given on the fixed-level problem and the transducer isomer splitting problem. Background on aptamers and antibodies is then given in background section. Discussion on engineering NTD transducers methods is given in discussion, following the Experimental Methods and Results sections describing critical tests on mode proliferation (or lack thereof) under strain conditions.

The fixed-level blockade problem

The bound state of the transducer/reporter molecule is sometimes found to not transduce to a different toggling ionic current flow blockade, but to a fixed-level blockade (i.e., the transducer provides distinctive channel modulation when unbound, but not so distinctive fixed-level channel blockades when bound [1]). It is important for both the bound and unbound transducers to have distinctive channel modulations in order to have automated high-precision state identification and tracking (and allow for multiplex assaying). In this instance, the switch to a fixed-level blockade was thought to be an effect of the large electrophoretically held complex forcing the channel-captured end to reside in one blockade state. This was previously explored in experiments where a streptavidin-coated magnetic bead was attached to biotinylated DNA hairpins known to be good modulators or poor channel modulators [10]. Once a streptavidin coated magnetic bead was attached to the biotinylated hairpins, it was found that gently pulsing the nanopore channel environment with a chopped laser beam (a laser-tweezer tugging) allowed a distinctive channel modulation to result (see Figure 4). It was found more recently that the induced blockade modulations occur in two types (chaotrope induced [5]; and laser-tweezer induced [10]). Further laser tweezer results showing the different, overlapping, modes will be given in the Results, where the experiments are performed with a DNA-hairpin transducer as in previous studies. In terms of the convenient Y-transducer, however, the same could be done by simply making use of the unused arm, as shown in Figure 5 (further see in Discussion).

In Figure 5 we use a Y topology with two arms (since one arm is to have a bead attachment). Stem length to nexus can be engineered to modulate when captured as before.

In Figure 5, the annealed Y-transducer is comprised of two, possibly LNA/RNA/DNA chimeric, nucleic acids, where the first single stranded nucleic acid is indicated by regions 1-3 and 7-8 and the second nucleic acid is indicated by regions 10-12. The paired regions {1,12}, {2,7}, and {8,11} are meant to be complements of one another (with standard Watson-Crick

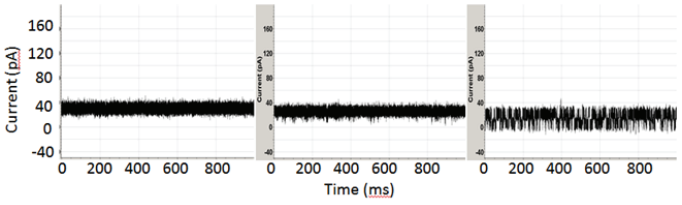

Figure 4: A (Left) Channel current blockade signal where the blockade is produced by a biotinylated 9GC DNA hairpin with 20 bp stem (9GC-biodT-ext).Reprinted with permission of Winters-Hilt S [10]. (Center) Channel current blockade signal where the blockade is produced by 9GC-ext-mag, the 9GC-biodT-ext molecule with magnetic bead attached. (Right) Channel current blockade signal where the blockade is produced by 9GC-biodT-ext with magnetic bead attached (9GC-ext-mag) and driven by a laser beam chopped at 4 Hz. Each graph shows the level of current in picoamps over time in milliseconds.

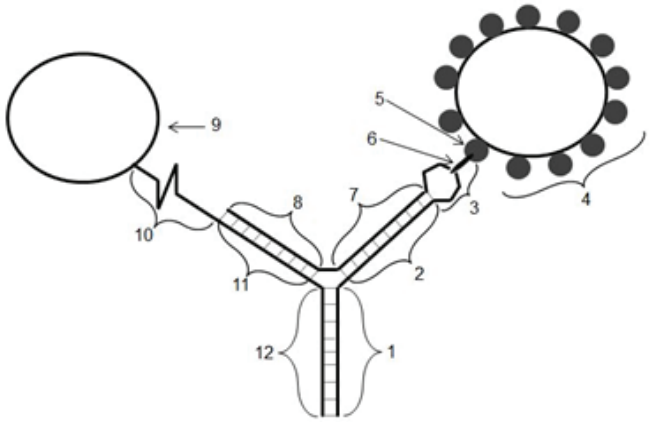

Figure 5: Y-laser transducer for high-specificity binding detection or individual protein binding/conformational change studies: Reprinted with permission of Winters-Hilt S [8]. The Y-transducer is meant to have a study molecule, region 9, attached by a single stranded nucleic acid linker, region 10, that is possibly a basic (non-base-pairing), that is linked to a single stranded nucleic acid region, region 11 & 12, that is meant to anneal to a second nucleic acid to create the Y-shaped nucleic acid construct shown.

base-pairing), and designed such that the annealed Y-transducer molecule is meant to be dominated by one folding conformation (as shown). Region 3 is a biotin-modified thymidine loop, typically 4-5 dT in size (here 5dT shown with 2 dT, a biotinylated dT, then another 2 dTs), that is designed to be too large for entry and capture in the alpha-hemolysin channel, such that the annealed Y-transducer only has one orientation of capture in the nanopore detector (without bead, region 4, attached). Region 4 is a streptavidin coated magnetic bead (that is susceptible to laser-tweezer impulses). The base region, comprising regions {1,9}, is designed to form a duplex nucleic acid that produces a toggling blockade when captured in a nanopore detector. The typical length of the base-paired regions is usually 8, 9 or 10 base-pairs. The study molecule (region 9), an antibody for example, has linkage to single stranded nucleic acid via a commoditized process due to the immuno-PCR industry so is an inexpensive well-established manufacturing approach for the molecular construction.

Transducer instability: short lifetime and isomer splitting under strain

Two twist conformations, due to different configurations in the hairpin loop and stem duplex conformation (such as B, B*, or A/B conformation duplex DNA), have been suspected from results on the DNA hairpins under other strain conditions, such as high voltage settings [1]. Thus, it is consistent that two types of DNA hairpin channel blockade modes appear in the laser-tweezer experiments. The two modes are thought to be rigid-body configuration changing, or 'toggling', and internal DNA hairpin configuration changing, or 'twisting'. Although the resulting toggle/twist mode signal analysis is more complicated when working with channel modulators, especially if induced by laser-tweezer, this is actually a highly favorable result since additional modulatory modes beyond the physically associated toggling and twisting are not seen. A bound transducer can now generically provide a modulatory state by use of a bead attachment with laser excitation, with high-strain modal proliferation apparently limited to two types, which is a very manageable situation given sufficient observation time. Thus, the stochastic carrier wave analysis [1] can proceed as before, only with more training data needed to 'learn' the more complicated background 'carrier wave' signal's characteristics. The transducer problem, thus, remains tractable with

laser-tweezer generalized (ubiquitous) transducer design. Furthermore, there is the ability to turn the twist mode type of internal signaling to our advantage in specialized transducer designs, as will be discussed in discussion section.

The problem with the DNA transducers with short lifetimes (in the electrophoretically-driven capture strain environment), and the internal mode transmission (excessive twist mode) transducers, is they have too much internal freedom. If it was possible to 'lock-up' some of the internal twist motion, then a stronger hairpin might result and one less likely to have twist modulations on top of toggle modulations. Such nucleic acid variants exist and are known as locked nucleic acid nucleosides (LNAs). They are a nucleic acid analogue where the ribose ring is locked into a highly favorable configuration for Watson-Crick base-pairing. The locking is accomplished by forming a methylene bridge from the 2'-O atom to the 4'-C atom of the ribose ring. LNA oligonucleotides can be synthesized using standard phosphoamidite chemistry (e.g., is compatible with standard enzymatic processes) and can be incorporated into chimeras with RNA and DNA [11]. The high affinity of LNA for complementary DNA or RNA provides improved specificity and stability, and is resistant to exonucleases and endonucleases for use in both *in vivo* and *in vitro* settings. The increased affinity leads to much more stable LNA hairpin and other LNA duplex configurations. This has special significance in the NTD setting where specially designed DNA hairpin and Y-transducer molecules have already been identified for use as event transduction molecules, and minor alterations on these transducers for the LNA form (see Methods) are obtainable that retain the transduction properties, but now with the long-lived and improved specificity and affinity attributes of LNAs [6]. LNA versions of the biotinylated hairpins explored where streptavidin binding occurs where one twist appears to dominate (so only toggle modes are non-trivial), and the lifetimes of the LNA/DNA chimeric transducer molecules in the high-strain capture environment of the nanopore is now on the order of hours instead of minutes [2,6,12].

The generic Y-transducer for annealing-based detection (no laser-tweezer needed) could have a form like in Figure 6, where the regions with high LNA content are shown in dashed boxes, protecting the molecule in those regions from terminus fraying, loop opening, or nexus opening.

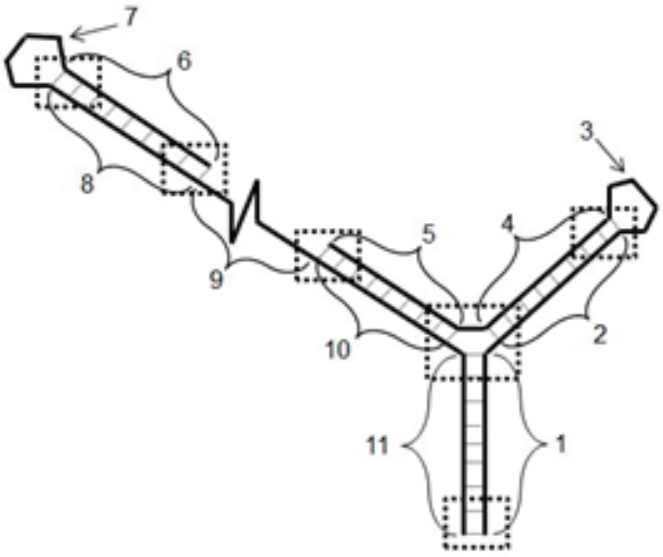

Figure 6: Y-transducer for annealing-detection for presence of specified viral digests: Reprinted with permission of Winters-Hilt S [8]. The boxed regions indicate favorable areas for LNA substitution to protect the molecule in those regions from base-pair fraying at the terminus, loop-opening, or nexus-branchings.

Background

The background in what follows focuses on the channel transducers. Background on the nanopore experiment [1,12,16] is not given in detail here since the focus is on engineering channel transducers.

Aptamer-based transducers: Aptamers are nucleic acids with high specificity and high affinity for a target molecule, the same properties found to be so useful in monoclonal antibody (mAb) diagnostics and biosensing applications. Aptamer selection is done by a rapid artificial evolutionary process known as SELEX. Nanopore-directed (NADIR) SELEX offers a means to accelerate the SELEX process and arrive at improved outcome, where the standard aptamer sequence library has the constraint that a portion of the sequence self-assemble (anneal) such that it provides an interface with a nanopore detector to provide a modulatory blockade and thereby introduce a 'stochastic carrier wave' (SCW) allowing a NADIR design/detection process [1,13]. Subject to the SCW constraint the bifunctional aptamer construct already satisfies the criteria to be a nanopore transduction reporter or event 'transducer'. If the transducer has a magnetic bead attachment 'arm', then we are now talking about a trifunctional molecule, thus the Y-shaped DNA molecule in the discussions that follow. Aptamer design can be quite complicated in some settings, however, such as when the binding target of interest involves large molecular features (for some air or water pollutants), large cell-surface features, heavy metal chelation binding, or because the aptamer transducer is inherently more complex with multiple binding moieties or functionalities. (See Disc. for examples of linked double-aptamer constructs and dual aptamer/antibody binding moieties. For the tissue-targeted antibody/aptamer quadfunctional transducer arrangements a 4-way, Holliday-junction, type of DNA molecule could be used, or a linkage via more complicated EDC linker technology [10].) The NADIR augmented SELEX procedure is even more advantageous in the more complicated aptamer design settings.

In Figure 7, the Center and Right Y-transducers are comprised of two, possibly RNA/DNA chimeric, nucleic acids, where the first single stranded nucleic acid is indicated by regions 1-5 (Center) or regions 1-6 (Right) and the second nucleic acid is indicated by regions 6-11 (Center) or 10-15 (Right). In the Left Figure, the paired regions {1,9}, {2,4}, and {5,8} are meant to be complements of one another (with standard Watson-Crick base-pairing), and designed such that the annealed Y-transducer molecule is meant to be dominated by one folding conformation (as shown). The region 3 is a loop, typically 4 dT in size, that is designed to be too large for entry and capture in the alpha-hemolysin channel, such that the annealed Y-transducer only has one orientation of capture in the nanopore detector. The base region, comprising regions {1,9}, is designed to form a duplex nucleic acid that produces a toggling blockade when captured in a nanopore detector. The typical length of the base-paired regions is 8-10 base-pairs.

Figure 8 [11] shows Y-transducer variations where the aptamer in Figure 7 Left is replaced with an antibody, while Figure 8 Right shows a variation in the Y-transducer where the base 'Y' conformation can be achieved with or without the binding target, and its nucleic acid attachment, needed to anneal to for the Y-transducer's stem region.

Antibody-based transducers and direct antibody glyco-profiling: Antibodies are the secreted form of a B-cell receptor, where the difference between forms is in the C-terminus of the heavy chain region. Figure 9 shows the standard antibody schematic. Standard notation is shown for the constant heavy chain sequence ('CH', 'H', and 'S' parts), variable heavy chain region ('VH' part), the variable light chain region ('VL' part), and constant light chain region ('CL' part). For a specific example, consider the equine IGHD gene [14] for the constant portion of the heavy chain, with exons corresponding with each of the sections CH1,H1,H2,CH2,CH3,CH4(S),

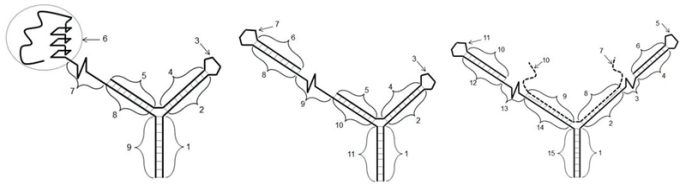

Figure 7: Left.Y-transducer for high-specificity aptamer binding detection. Center and Right: Y-transducers for testing hypothesized miRNA binding sites and/or miRNA interactions with a known miRNA binding site: The Y-transducer is meant to have a high-specificity aptamer attached by a single stranded, possibly a basic (non-base-pairing), nucleic acid linker, region 7, to an aptamer in region 6. The sketch of the aptamer in region 6 is meant to suggest the 3D conformational aspect of the aptamer, where stacking of G-quadruplexes is a common, but not necessary, feature of aptamers.

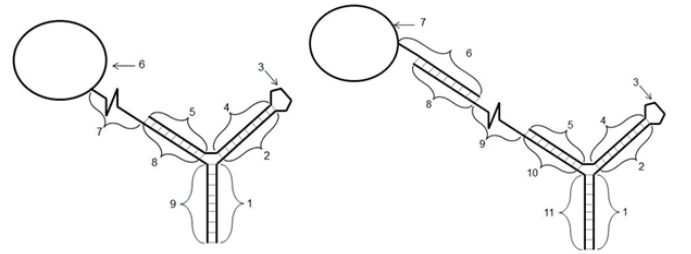

Figure 8: Y-transducer for high-specificity antibody binding detection.

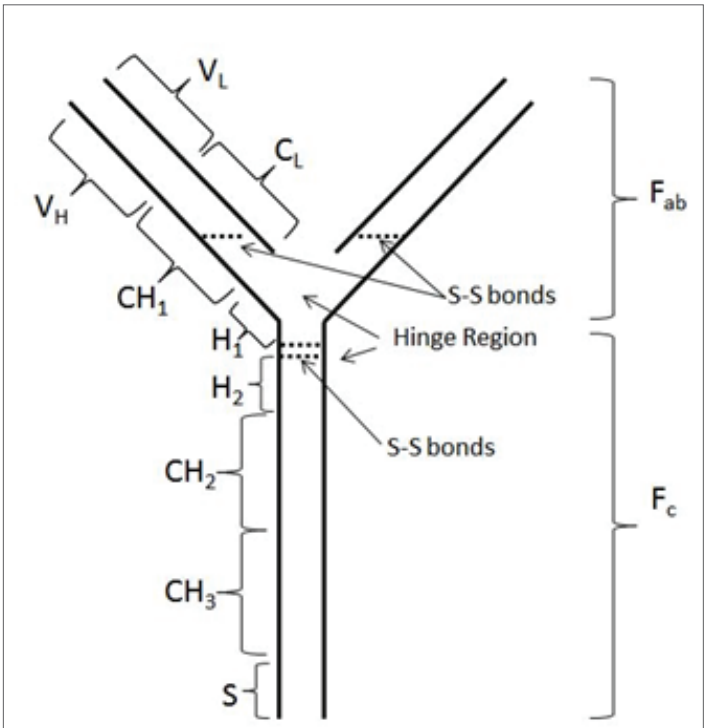

Figure 9: The standard antibody schematic: Reprinted with permission of Karlsen KK [11]. Standard notation is shown for the constant heavy chain sequence ('CH', 'H', and 'S' parts), variable heavy chain region ('VH' part), the variable light chain region ('VL' part), and constant light chain region ('CL' part). The full heavy chain sequence is derived from recombination of the VH part and {CH,H,S} parts (where the secretory region S is also called CH4).

and for the membrane-bound form of IGHD, there are two additional exons, M1 and M2 for the transmembrane part, thus, CH1, H1, H2, CH2, CH3, CH4(S), M1, M2. In Figure 9, the long and short chains are symmetric from left to right, their glycosylations, however, are generally not symmetric. Critical di-sulfide bonds are shown connecting between chains, each of the VH and CH regions typically have an internal disulfide bond as well. The lower portion of the antibody is water soluble and can be crystallized (denoted Fc). The upper portion of the antibody is the antigen binding part (denoted Fab).

Figure 10 shows a typical antibody N-glycosylation (exact example for equine IGHD [14]). N-glycosylation consists of a covalent bond (glycosidic) between a biantennary N-glycan (in humans) and asparagine (amino acid 'N', thus N-glycan). The covalent glycosidic bond is enzymatically established in one of the most complex post translational modifications on protein in the cell's ER and Golgi organelles, and usually only occurs in regions with sequence "NX(S/T) – C-terminus" where X is 'anything but proline' and the sequence is oriented with the C-terminus as shown. Licensed therapeutic antibodies typically display 32 types of biantennary N-glycans [15-20], consisting of N-acetyl-glucosamine residues (GlcNAc, regions '1'); mannose residues (Man, regions '2'); galactose residues (Gal, regions '3'), and Sialic Acid Residues (NeuAc, regions '4'), as shown in Figure 10. The N-glycans are classified according to their degree of sialylation and number of galactose residues: if disialylated (shown) have A2 class. If asymmetric and monosialylated have A1 class. If not sialylated then neutral (N class). If two galactose residues (shown) then G2 class, if one, then G1 class, if zero, then G0 class. If there is an extra GlcNAc residue bisecting between the two antennae +Bi class (–Bi shown). If a core fructose is present (location near GlcNAc at base) then +F (–F shown). So the class shown is G2-A2. The breakdown on the 32 types is as follows: 4 G2-A2; 8 G2-A1; 4 G1-A1; 4 G2-A0; 7 G1-A0; 4 G0-A0 [20]. The N-glycans with significant acidity (A2 and A1) are 16 of the 32, so roughly half of the N-glycans enhance acidity. The other main glycosylation, involving O-glycans, occurs at serine or threonine (S/T). The main non-enzymatic glycations occur spontaneously at lysines ('K') in proteins in the blood stream upon exposure to glucose via the reversible Maillard reaction to form a Schiff Base (cross-linking and further reactions, however, are irreversible and associated with the aging process).

The base of the antibody plays the key role in modulating immune cell activity. The base is called the Fc region for 'fragment, crystallizable', which is the case, and to differentiate it from the Fab region for 'fragment, antigen-binding' that is found in each of the arms of the Y-shaped antibody molecule. The Fc region triggers an appropriate immune response for a given antigen (bound by the Fab region). The Fab region gives the antibody its antigen specificity; the Fc region gives the antibody its class effect. IgG and IgA Fc regions can bind to receptors on neutrophils and macrophages to connect antigen with phagocyte, known as opsonization (opsonins attach antigens to phagocytes). This key detail may explain the modulatory antibody interaction with the nanopore channel. IgG, IgA, and IgM can also activate complement pathways whereby C3b and C4b can act as the desired opsonins. The C-termini and Fc glycosylations of an antibody's heavy chain, especially for IgG, is thus a highly selected construct that appears to be what is recognized by immune receptors, and is evidently what is recognized as distinct channel modulator signals in the case of the NTD (mAb channel blockade signals are shown in Figure 11 and Figure 12 from [10]). Using NTD we can co-opt the opsonization receptor-binding role of the Fc glycosylations (and mAb glycations and glycosylations in general), and the C-terminus region, to have a channel modulating role. This may also permit a new manner of study of the critical opsonization role of certain classes of antibodies (and possibly differentiate the classes in more refined ways) by use of the nanopore detector platform. The channel may also provide a means to directly measure and characterize

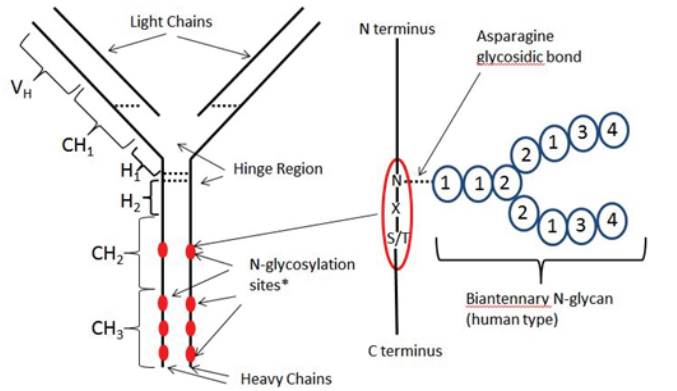

Figure 10: Typical antibody N-glycosylation: Reprinted with permission of Karlsen K.K [11]. A schematic for typical antibody N-glycosylation is shown (drawn from results on the equine IGHD gene [14]), where one possible N-glycosylation site is indicated in region CH2, and three possible N-glycosylation sites are indicated in region CH3.

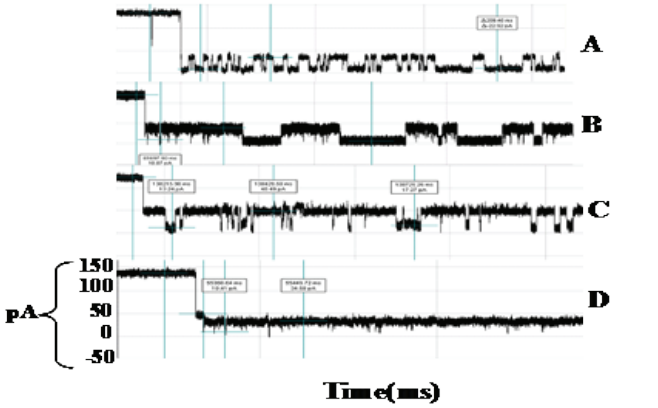

Figure 11: Multiple Antibody Blockade Signal Classes: Reprinted with permission of Winters-Hilt S [10]. One second traces of the various IgG region captures and their associated toggle signals: the four most common blockade signals produced upon introduction of a mAb to the nanopore detector's analyte chamber (the cis-channel side, typically with negative electrode). Other signal blockades are observed as well, but less frequently or rarely.

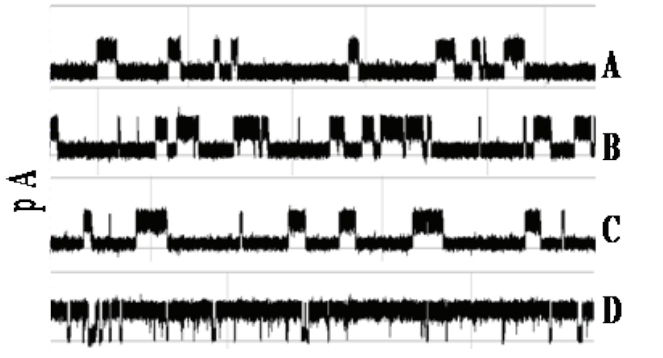

Figure 12: Antibody-Antigen binding – clear example from specific capture orientation: Reprinted with permission of Winters-Hilt S [10].Each trace shows the first 750 ms of a three minute recording, beginning with the blockade signal by an antibody molecule that has a portion inserted into the alpha-hemolysin channel to produce a toggle signal (A). Antigen is introduced at the beginning of frame A (100 μg/ml of 200 kD multivalent synthetic polypeptide (Y,E)-A—K). By frame D we see a transition to a new type of blockade that is not seen without introduction of antigen.

antibody Fc glycosylations, a critical quality control needed in antibody therapeutics to have correct human-type glycosylation profiles in order to not (prematurely) evoke an immunogenic response.

A preliminary analysis of antibody blockade studies on the nanopore detector, for a well defined synthetic polypeptide antigen, has been done [4,21]. Similar results are found for IgG subclass 1 monoclonal antibodies for biotin, HIV, and anti-GFP, and all have produced the desired modulatory signals to have a NTD transducer. The critical role of Fc glycosylation has already been mentioned, but there is also the critical role in understanding antigen-antibody binding in the Fab region. Hydrophobic bonds are very difficult to characterize by existing crystallographic and other means, and often contribute half of the overall binding strength of the antigen-antibody bond [4,12]. Hydrophobic groups of the biomolecules exclude water while forming lock and key complementary shapes. The importance of the hydrophobic bonds in protein-protein interactions, and of critically placed waters of hydration, and the complex conformational negotiation whereby they are established, may be accessible to direct study using nanopore detection methods. Further work on antibody studies is beyond the scope of this paper, however, and will be presented elsewhere.

Methods

Nanopore Detector Experiments

Each experiment is conducted using one alpha-hemolysin channel inserted into a diphytanoyl-phosphatidylcholine/hexadecane bilayer across a, typically, 20-micron-diameter horizontal Teflon aperture. The alpha-hemolysin pore has a 2.0 nm width vestibule opening allowing a dsDNA molecule to be captured (while as DNA molecule translocates). The effective diameter of the bilayer ranges mainly between 1-25 μm. This value has some fluctuation depending on the condition of the aperture, which nanopore station is used, and the bilayer applied on a day to day basis. Seventy microliter chambers on either side of the bilayer contain 1.0 M KCl buffered at pH 8.0 (10 mM HEPES/KOH) except in the case of buffer experiments where the salt concentration, pH, or identity may be varied. Voltage is applied across the bilayer between Ag-AgCl electrodes. DNA control probes are typically added to the cis chamber at 10-20 nM final concentration. All experiments are maintained at room temperature (23 ± 0.1 °C), using a Peltier device.

NTD control probes

The five DNA hairpins that have been carefully characterized previously [22,23], are used as highly sensitive controls (obtained from IDT DNA with PAGE purification). The nine base-pair hairpin molecules share an eight base-pair hairpin core sequence, with addition of one of the four permutations of Watson-Crick base-pairs that may exist at the blunt end terminus, i.e., 5'-G|C-3', 5'-C|G-3', 5'-T|A-3', and 5'-A|T-3'. Denoted 9GC, 9CG, 9TA, and 9AT, respectively. The full sequence for the 9GC hairpin is 5'-GTTCGAACGTT TTCGTTCGAAC-3'. The eight base-pair DNA hairpin (8GC) is identical to the core eight base-pair part of the 9GC sequence, except the terminal base-pair is changed to be 5'-G|C-3' (e.g., 5'-GTCGAACGTT TTCGTTCGAC-3'). Each hairpin was designed to adopt one base-paired structure.

NTD transducers

NTD Y-transducer/Reporter probe: The Y-shaped NTD-transducer molecule design used in the SNP experiments [1,4], and referenced in the Discussion, has a three-way DNA nexus geometry: 5'-CTCCGTCGAC GAGTTTATAGAC TTTT GTCTATAAACTC GCAGTCATGC TTTT GCATGACTGC GTCGACGGAG-3'. Two of the junctions' arms terminate in a 4T-loop and the remaining arm, of length 10 base-pairs, is usually designed to be blunt ended. The blunt ended arm, or 'stem', has been designed such that when it is captured by the nanopore it produces

a toggling blockade. The Y-transducer can be linked with aptamer-based therapeutics [24-28] as will be discussed in discussion.

Biotinylated DNA transducers (from IDT DNA, purification by PAGE):

8GC-BiodT: 5'- GTCGAACGTT/iBiodT/TTCGTTCGAC -3'

9GC-BiodT: 5'- GTTCGAACGTT/iBiodT/TTCGTTCGAAC -3'

Biotinylated LNA/DNA Chimeric transducers (from Exiqon, purification by HPLC): 8GC-BiodT: 5'- +G+TCGAA+C+GTT/iBiodT/TT+CGT+T+CG+AC -3'. The LNA version of 8GC-Bt has 8 LNA bases shown preceded by '+', 12 DNA bases, and 1 biotin dT base.

9GC-BiodT: 5'- +G+CTTGAA+C+GT/iBiodT/TT+CGTT+CAA+GC -3'. The LNA version of 9GC-Bt stem does not have the same sequence as the DNA-based 9GC, and has only a 3dT loop aside from the modified dT with biotin attachment, and has 7 LNA bases shown preceded by '+', 14 DNA bases, and 1 biotin dT base.

Laser Trappingtransducers (from IDT DNA, purification by HPLC): The 20bp hairpin with 4dT loop: 9GC-ext:

5'- GTTCGAACGGGTGAGGGCGCTT TTGCGCCCTCACCCGTTCGAAC -3'

The 20bp hairpin with 5dT loop , where the central loop dT was modified to have a linker to biotin: 9GC-BiodT-ext:

5'-GTTCGAACGGGTGAGGGCGCTT/iBiodT/TTGCGCCCTCACCCGTTCGAAC -3'

Conjugation to Magnetic Beads

The streptavidin-coated magnetic bead diameters were approximately 1 micron and the mass about 1 pg. Some of the bead preparations involved use of bovine serum albumin (BSA) buffer, which required tolerance of BSA at the nanopore detector. This was separately confirmed for the concentrations of interest, up to the level of 8mg/mL BSA [6].

Laser Setup

Laser illumination provided by a Coherent Radius 635-25. Output power before fiber optic was 25mW at a wavelength of 635 nm. The beam was chopped at 4Hz. During laser excitation studies the Faraday cage was removed. Significant 60 Hz wall-power noise was not seen with cage removed when there was no laser illumination, but with cage removed and under laser illumination 60Hz line noise could clearly be seen. The 60 Hz line noise was, thus, picked up at the laser's power supply and transmitted via the laser excitation process into the detector environment as a separate modulatory source. After fiber optic, approximately 5-10mW illumination is focused into in an approximate 1mm illumination diameter produced at the nanopore detector's aperture.

Data acquisition and FSA-based Signal acquisition

Data is acquired and processed in two ways depending on the experimental objectives: (i) using commercial software from Axon Instruments (Redwood City, CA) to acquire data, where current was typically filtered at 50 kHz bandwidth using an analog low pass Bessel filter and recorded at 20 μs intervals using an Axopatch 200B amplifier (Axon Instruments, Foster City, CA) coupled to an Axon Digidata 1200 digitizer. Applied potential was 120 mV (*trans*side positive) unless otherwise noted. In some experiments, semi-automated analysis of transition level blockades, current, and duration were performed using Clampex (Axon Instruments, Foster City, CA). (ii) using Lab View based experimental automation. In this case, ionic current was also acquired using an Axopatch 200B patch clamp amplifier (Axon Instruments, Foster City, CA), but it was then recorded using a NI-MIO-16E-4 National Instruments data acquisition card (National Instruments, Austin TX). In the Lab View format, data was low-pass filtered by the amplifier unit at 50 kHz, and recorded at 20 μs intervals. Signal acquisition from the 20 μs sample stream was done using a Finite State Automaton (FSA) [1,22,29].

Machine Learning based Signal Processing

With completion of Finite State Automata (FSA) preprocessing, and hidden Markov model (HMM) filtering to remove noise from the acquired signals, and to extract features from them. The HMM in one configuration (for control probe validation) is implemented with fifty states, corresponding to current blockades in 1% increments ranging from 20% residual current to 69% residual current [1,22]. The HMM states, numbered 0 to 49, corresponded to the 50 different current blockade levels in the sequences that are processed. The state emission parameters of the HMM are initially set so that the state j, $0 <= j <= 49$ corresponding to level $L = j+20$, can emit all possible levels, with the probability distribution over emitted levels set to a discretized Gaussian with mean L and unit variance. All transitions between states are possible, and initially are equally likely. Each blockade signature is de-noised by 5 rounds of Expectation- Maximization (EM) training on the parameters of the HMM. After the EM iterations, 150 parameters are extracted from the HMM. The 150 feature vectors obtained from the 50- state HMM-EM/Viterbi implementation are: the 50 dwell percentage in the different blockade levels (from the Viterbi trace-back states), the 50 variances of the emission probability distributions associated with the different states, and the 50 'merged' transition probabilities from the primary and secondary blockade occupation levels. By merged is meant taking the transition probabilities from the dominant blockade level and to add them component-wise with the transition probabilities from the second most dominant level, which works well for compression for two-state dominant modulatory blockade signals. Variations on the HMM 50 state implementation are made as necessary to encompass the signal classes under study.

The 150-component feature vector extracted for each blockade signal is then classified using a trained Support Vector Machine (SVM). The SVM training is done off-line using data acquired with only one type of molecule present for the training data (bag learning) [1,22].

For experiments with pattern recognition informed (PRI) sampling, a channel blockade capture signal is filtered and amplified before it is sent through the DAQ. The first 200 ms detected after drop from baseline are sent via TCP-IP protocol to the HMM software, which generates a profile for each signal sent. The HMM-generated profile is processed with the SVM classifier to determine whether the signal is acceptable. If the signal is acceptable, the message to continue recording is sent to the Lab Windows software to continue recording, and the molecule is not ejected from the channel by the amplifier. If not, the amplifier briefly reverses the polarity to eject the molecule from the channel. The nanopore experiments with PRI sampling are done with a 1:70 mixture of 9GC:9TA [9].

Albumin can intercalate into the bilayer (cholesterol also) and initially this strengthens the bilayer and lowers the system RMS current noise, but eventually there is too much of a good thing and the albumin is probably agglomerating and causing bilayer disruption, which, in turn, can compromise the entire experiment. There are a variety of buffer modifications that can be introduced that are protective of the bilayer, including blocking the albumin intercalation. In doing so, however, new interference molecules are introduced that can damage the channel. It is observed, however, that the new interference problem is only a problem if the protocol is non-responsive, e.g. if the blockade is not recognized as a 'bad' blockade and ejected promptly (if not ejected promptly the molecule gets 'stuck'). An auto-eject cycle can be used that is set to whatever minimal observation time is needed per blockade in the experiment of interest, to help mitigate bad signal issues. It is found that good and bad signal recognition can aid operations. Generally any signal that is modulating is

good, so if the rule is adopted that a signal is rejected if non-modulatory in its first 0.5 seconds, this provides is a pretty good operational setting. The PRI sampling can thus be employed, indirectly, to provide channel protection and maintain operational status for prolonged periods. In this paper signal processing was only critical for the aforementioned PRI-based channel protection. So the Results that follow are of a qualitative nature on the number of signal mode types and not a quantitative signal analysis of the histogram profiles of the blockade signals [1,12,16].

Results

Indications of Twist modes

Experiments are done with biotinylated DNA20bp hairpins (9GC-biodT-ext) that are linked to streptavidin-coated magnetic beads (forming (GC-ext-mag) in pH 8 buffer. The transducer DNA hairpin has stem length twenty base-pairs (20bp) and loop size 5 dT, with the central thymidine modified with a linker to biotin. The hairpin in this form is referred to as 9GC-biodT-ext because it is a 20bp extension of the biotinylated 9GC control molecule that has a 9bp stem. The hairpin is then mixed with a solution of magnetic beads that have a streptavidin coating, leading to complexes of magnetic beads attached to a DNA hairpin channel modulator (9GC-ext-mag) by way of a streptavidin-biotin linkage. The mass of the magnetic bead is substantially greater than the hairpin, such that upon capture the likelihood of twist mode being excited is even greater (an even greater angular momentum impulse would occur on capture), even though it is still relatively rare initially. As the experiment proceeds, however, the twist modulating captures increase in likelihood due to more beads becoming more bound with hairpin and thus more mass and charge, thus greater angular momentum impulse on capture (Figure 13).

Laser-tweezer pulsing has been found to induce a transition from a fixed-level to a toggling blockade on biotinylated 20bp DNA hairpins [10]. It was not clear at that time however, that there was both spatial configuration switching and twist configuration switching, because the latter switching hadn't been seen before. The existence of two loop/stem twist configurations began to become apparent, however, as experiments began to explore a variety of strain conditions, such as high urea (such as 2-5M concentration of chaotrope, see Figure 3) [5], higher than the 120 mV applied potential (such as 150-180 mV), higher pH (9 or greater), or in the presence of large bound charge/mass objects (e.g., streptavidin, streptavidin-bead, antibody, or large-antigen attachment).

In Figure 14, we see a channel blockade due to 9GC-ext-mag in the presence of laser-tweezer pulsing (using a chopped laser beam focused with an off-target edge-illumination intensity gradient). The upper 'twist-level' is briefly seen (the 42pA level), followed by a switch to the lower-level twist blockade that has its own, laser-induced, toggle, before sticking at the lower twist state's lower blockade level at the end of the trace (the sticking could be due to the magnetic bead attaching other biotinylated hairpins with increase in charge and overall electrophoretic driving force). The image on the Right in Figure 14 is an enlarged view of the lower twist state's laser induced toggle as it finally becomes 'stuck' at one level. Note the clear 60 Hz line noise evident in the enlarged view. This noise is not present in 9GC-ext-mag blockades without laser illumination (and without cage), so the 60Hz line noise is being transmitted in the laser beam not via the unshielded surroundings. The laser was found to induce the most notable switching in the lower-level twist state when chopped at 4Hz.

Clearly the twist toggle adds complication on top of the spatial configuration-toggle and this impacts the design of the transducers. Use of LNAs to lock the twist configuration is expected to eliminate the loop-stem twist toggle complication, but it's not as if the signal processing can't

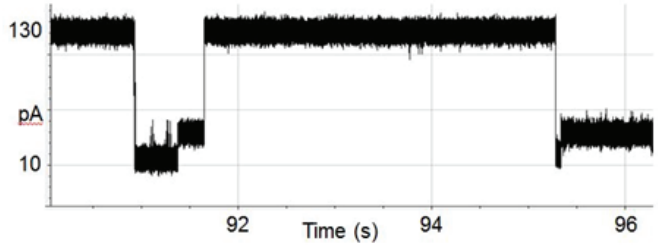

Figure 13: A less common, short duration, full-length 9GC-ext-mag blockade signal is shown (before diffusional escape) with the beginning of another at far right. The Faraday cage is in-place for this trace, and the 42pA level is seen as before as the upper level toggle (but is less noisy than before since the cage in place). Two clear levels of blockade can be seen, and are thought to correlate with two distinct molecule-channel blockade configurations/conformations as usual. The toggle signals are thought to describe a switching between molecular loop/stem 'twist' conformations, however, and not between two channel blockade configurations (where the molecule in the same internal conformation).

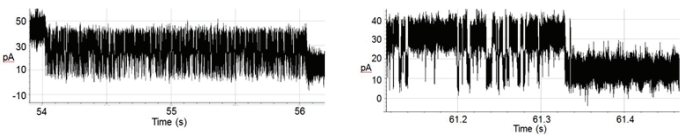

Figure 14: Left.A 9GC-ext-mag blockade signal with Laser-Tweezer modulation (no cage): The upper-level twist state is now at ~45pA, and the lower-level twist state itself toggles between 30pA and 15pA (with fraying 'spikes' to 0pA as seen in other hairpin studies [22,23]). Right: Enlarged view of lower-level twist toggling, then sticking at its lower level (note the 60Hz noise is from the laser; without laser, but no cage, there is no 60Hz noise). The beam chopper frequency is 4Hz, but the 'awakened' stochastic modulation is non-periodic.

manage the two-toggle mode signal for most cases. So, the main purpose in tuning the LNA content in the LNA/DNA chimeras is to select the most effective transmission of binding event to the channel modulator, where most effective could be via twist mode transmission with large-mass long-tether via a long DNA arm (Figures 15 and 16), while for low-mass short-arm tethering linkages the most effective transducer may require a very rigid LNA/DNA chimera (lots of LNA).Further results on twist modes and long-lifetime LNA/DNA chimeric transducers [6], are beyond the scope of this paper so will only be discussed as needed.

Discussion

Transducer design with aptamer or antibody, with possible magnetic bead attachment

When working with longer stem-length DNA hairpin captures the duplex end is observed to mainly reside in one, fixed, blockade configuration [4], probably due to the electrophoretic force strongly drawing the larger charge nucleic acid into the channel. In early tests with annealing a fixed blockade states often weren't a problem with the Y-shaped transducers, especially for the unbound case, but became a complication when bound if the bound object was 'large' or a significant length of nucleic acid, or when working with a commoditized linkage by annealing to an immuno-PCR tagged antibody or other protein. When working with longer DNA hairpins with large mass/charge attachments sometimes the opposite occurred, the large bound extension appeared to induce occasional toggling where none was observed before (such as seen in streptavidin-coated bead binding to biotinylated 20bphp hairpins [6]). In order to have a controlled way to have a simple nucleic acid based transducer, it was then attempted to

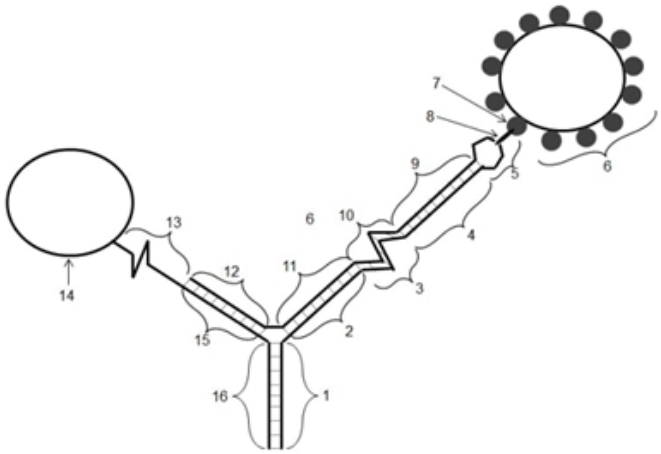

Figure 15: Y-transducer for single molecule studies using twist mode modulations: Reprinted with permission of Karlsen KK [11]. Region 14 indicates the study molecule of interest (an antibody for antibody-detection or a protein for conformation/binding studies), where a magnetic bead is attached for laser-tweezer modulation (region 6), where the transducer is designed with sufficient LNA substitutions to allow laser-tweezer excitations to be transmitted as a twist-mode impulse (shown in regions numbered {3,10}) while maintaining discernibly different signals according to the study molecules state. In Fig. 15, paired regions {1,16}, {2,11},{4,9},{12,15} are designed to anneal with the dominant conformation shown, and are typically a minimum of 8 or 9 base-pairs in length. The linker arm in Region 13 and Region {12,15}, is whatever is needed to provide sufficient steric clearance between region 14 and region 6 when the stem (region {1,16}) is captured and held at the nanopore.

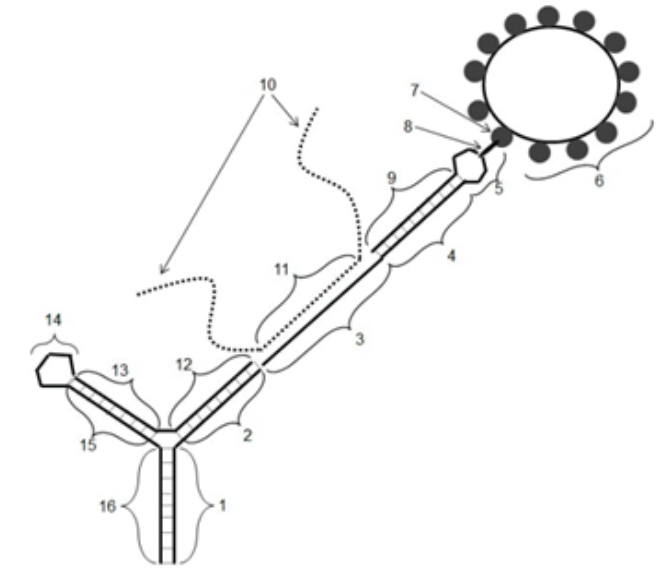

Figure 16: Y-transducer for single molecule annealing studies using twist mode modulations: Reprinted with permission of Karlsen KK [11]. Region 10 indicates the single stranded nucleic acid study molecule of interest: a nucleic acid whose region 10 section is annealed to region 3 of the transducer; where a magnetic bead is attached for laser-tweezer modulation (region 6), where the transducer is designed with sufficient LNA substitutions to allow laser-tweezer excitations to be transmitted as a twist-mode impulse through the annealed-target region. A twist mode will only transmit if the annealing-target is bound, giving rise to very different channel modulation signals.

recover unique modulatory blockade signaling by linking to a magnetic bead where laser-tweezer 'tugging' could then be used for injection of kinetic energy at the single molecule level [10]. Initial results indicated the possibility for a simple inexpensive probe design, as described in what follows, but it was unclear if the stochastic carrier wave signal processing on the more complex transducer modulation signal would be possible given the proliferation in blockade modes observed under laser-tweezer modulation. In more recent studies with chaotropes, the isoforms of the DNA hairpin modulators is better understood, however, indicating that there are two mode types of modulation in captured duplex nucleic acid: position/orientation and twist/stretch, where the new signal complication is due to the appearance of the twist/stretch modes. Since there is just the one new mode class for duplex nucleic acid channel blockade (twist modes), the mode proliferation is limited, and SCW signal processing can be performed.

So, nanopore-captured DNA hairpin modulators can exhibit not only spatial/orientation toggling but also torsional/twisting toggling when sufficiently excited. This effect becomes most notable when channel modulations are induced by laser-tweezer pulsing. The new understanding of the laser-tweezer induced modulations suggests a limit for the induced modulator's signal classes to those already seen and a manageable signal analysis platform can thereby be implemented. In practice a stochastic channel modulator that produces the simplest, non-fixed-level, stationary signal blockade is desired, such that the stochastic carrier wave (SCW) signal processing methods can be employed. The position and twist toggle modes in the modulator together pose a more complex SCW system, but can be managed with sufficient sample observations on modulator during its different states (such as linked to bound or unbound analyte). As mentioned earlier, a related complication with using DNA-based channel modulators has been their short lifetimes until melting. This problem was eliminated by use of locked nucleic acid nucleosides (LNAs) in applications involving isomers [6], where LNAs serve to reduce twist modes by locking the nucleic acid and thereby restricting its internal degrees of freedom in term of twist/stretch. This can be a good thing in that it will simplify the SCW signal training mentioned above. A simpler SCW analysis is not critical, however, as long as the SCW learning can be done with a manageable amount of training data. So the main optimization to be accomplished by 'locking up' the modulator with increased LNA is effectively a tuning over molecular variants with greater or lesser twist mode event transmission. For annealing-based detection this could be critical since the properly annealed nucleic acid duplex will transmit twist mode excitations notably differently than improperly annealed DNA (if even present). For this reason some modulator arrangements with laser-tweezer pulsing may have their bead attachment on the same arm as the annealing binding site (see Figures 15 and 16), and have a low number of LNA bases in the LNA/DNA chimeras in the binding template (keeping blunt terminus and Y-nexus regions strongly LNA based to prevent melting as much as possible, but permitting twisting). In Figure 15 a description is given for a Y-transducer for single molecule studies using twist mode modulations. A 'twist mode' specialized Y-transducer for single molecule annealing studies using twist mode modulations is shown in Figure 16. Figure 17 shows a 4-way transducer (a.k.a, a Holliday Junction transducer), for dual aptamer/antibody tissue-targeting functional aptamer delivery studies [24-28], where a modulatory transducer is enabled by laser-tweezer coupling.

In Figure 16, paired regions {1,16}, {2,12},{4,9},{13,15} are designed to anneal with the dominant conformation shown, and are typically a minimum of 8 or 9 base-pairs in length. The loop in Region 14 is designed to not favor channel capture and strongly favor a single conformation for the Region 13-15 stem-loop region.

The Y-shaped DNA transduction molecule is also a versatile construct to test for as an intermediate annealed complex (see single nucleotide polymorphism SNP detection efforts [4] for further details). Highly accurate SNP detection with the Y-shaped DNA transduction molecule was found to be possible by designing the Y-transducer to anneal to nucleic acid target sequence such that the SNP variant occurs in the Y-nexus region [4], giving rise to a clear difference in the annealed Y-transducer's channel modulation. The NTD method provided a means to perform SNP variant detection to very high accuracy that will likely be improved further when using the higher specificity LNA form of the transducers [6,12].

Chelator design, and targeted therapeutic aptamer delivery design

Functionalizing both Y-transducer arms for binding actually leads to a number of other options, such as double aptamer molecules (see Figure 18 for possible use in heavy metal chelation), dual aptamer/antibody transducers (see Figure 19, used in tumor-directed aptamer delivery), where two drugs are FDA approved of this type [24-28], and dual DNA annealing testing (see Figure 19).

In Figure 18, the Y-transducer is comprised of three, possibly RNA/DNA chimeric, nucleic acids, where the first single stranded nucleic acid is indicated by regions 1-4, the second single stranded nucleic acid is indicated by regions 5 and 6, and the third nucleic acid is indicated by regions 7-10. The paired regions {1,10}, {2,5}, and {6,9} are meant to be complements of one another (with standard Watson-Crick base-pairing), and designed such that the annealed Y-transducer molecule is meant to be dominated by one folding conformation (as shown). The base region, comprising regions {1,10}, is designed to form a duplex nucleic acid that produces a toggling blockade when captured in a nanopore detector. The typical length of the base-paired regions is usually 9 or 10 base-pairs. The same Y-transducer is shown on the right, but with a binding target, object 11, positioned for a chelation-type binding configuration, this in addition to any possible chelation binding on the part of the individual aptamers during their individual binding to object 11.

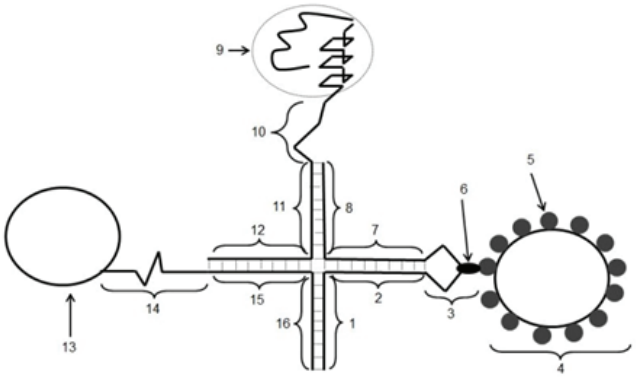

Figure 17: A 4-way transducer (a.k.a, a Holliday Junction transducer): Used for dual aptamer/antibody tissue-targeting functional aptamer delivery studies, where a modulatory transducer is enabled by laser-tweezer coupling.

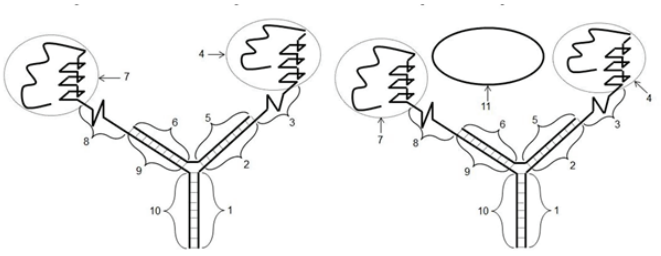

Figure 18: Left and Right: Y-transducer for high-specificity dual-aptamer binding detection: The Y-transducer shown on the left is meant to have two high-specificity aptamers attached by single stranded, possibly abasic (non-base-pairing), nucleic acid linkers, with region 8 for the left arm linker to the left arm aptamer in region 7 and region 3 for the right arm linker to the right arm aptamer in region 4. The sketch of the aptamers in regions 4 and 7 is meant to suggest the 3D conformational aspect of the aptamer, where stacking of G-quadruplexes is a common, but not necessary, feature of aptamers.

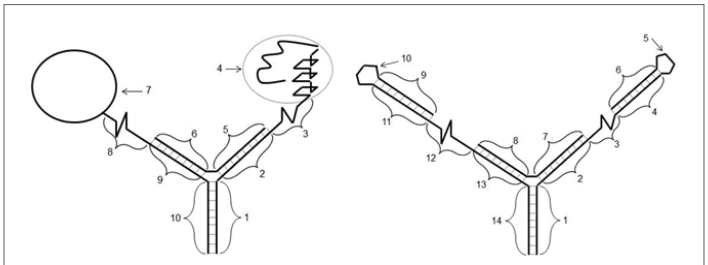

Figure 19: Left and Right: Y-transducer for high-specificity dual aptamer/antibody binding detection; and Y-transducer for dual testing for presence of specified viral digests.

Conclusion

Two types of DNA hairpin channel blockade modes appear in the laser-tweezer experiments. The two modes are thought to be rigid-body configuration changing, or 'toggling', and internal DNA hairpin configuration changing, or 'twisting'. By use of LNA/DNA chimeras with varying amounts of LNA, the twist modes can be locked out. Melting times on the transducers can be directly designed similarly. High-strain bound transducers can thus be used with a modulatory state by use of a bead attachment with laser excitation, with high-strain modal proliferation limited to two types (in the results seen thus far). Using stochastic carrier wave analysis with sufficient training data to 'learn' the transducer's 'carrier wave' signal characteristics, a stable NTD biosensing platform can be then established. The transducer problem, thus, appears to be solvable with laser-tweezer generalized (ubiquitous) transducer design involving LNA/DNA-chimeric transducers.

Acknowledgements

The author would like to thank META LOGOS Inc., for research support and a research license. The author would like to thank the Meta Logos nanopore technicians Eric Morales, Joshua Morrison, Evenie Horton, and early work by the nanopore technicians based out of the SWH Lab at Children's Hospital New Orleans: Amanda Alba and Andrew Duda.

References

1. Winters-Hilt S (2011) Machine-Learning based sequence analysis, bioinformatics & nanopore transduction detection. ISBN: 978-1-257-64525-1.
2. Winters-Hilt S, Horton-Chao E, Morales E (2011) The NTD Nanoscope: potential applications and implementations. BMC Bioinformatics 12 Suppl 10: S21.
3. Thomson K, Amin I, Morales E, Winters-Hilt S (2007) Preliminary nanopore cheminformatics analysis of aptamer-targetbinding strength. BMC Bioinformatics 8Suppl7:S11.
4. Winters-Hilt S (2007) The α-Hemolysin nanopore transduction detector – single-molecule binding studies and immunological screening of antibodies and aptamers. BMC Bioinformatics 8 Suppl7: S9.

5. Winters-Hilt S, Stoyanov A (2016) Nanopore Event-Transduction Signal Stabilization for Wide pH Range under Extreme Chaotrope Conditions. Molecules 21: 346.

6. Winters-Hilt S (2017) Isomer-specific trace-level biosensing using a nanopore transduction detector.

7. Winters-Hilt, S, Davis A, Amin I, Morales E (2007) Nanopore current transduction analysis of protein binding to non-terminal and terminal DNA regions: analysis of transcription factor binding, retroviral DNA terminus dynamics, and retroviral integrase-DNA binding. BMC Bioinformatics 8 Suppl 7: S10.

8. Winters-Hilt S (2016) Exploring protein conformation-binding relationships and antibody glyco-profiles using a nanopore transduction detector. Mol And Med Chem 2: e1378.

9. Eren AM, Amin I, Alba A, Morales E, Stoyanov A, et al. (2010) Pattern Recognition Informed Feedback for Nanopore Detector Cheminformatics. Adv Exp Med Biol 680: 99-108.

10. Winters-Hilt S (2006) Nanopore Detector based analysis of single-molecule conformational kinetics and binding interactions. BMC Bioinformatics 7Suppl 2: S21.

11. Karlsen KK, Wengal J (2012) Locked Nucleic Acid and Aptamers. Nucl.Acid Ther 22: 366–370.

12. Winters-Hilt S (2017) Biological system analysis using a nanopore transduction detector: from miRNA validation, to viral monitoring, to gene circuit feedback studies.

13. Winters-Hilt S (2017) Channel current Cheminformatics and Stochastic Carrier-Wave signal processing.

14. Wagner B, Miller DC, Lear TL, Antczak DF (2004) The Complete Map of the Ig Heavy Chain Constant Gene Region Reveals Evidence for Seven IgG Isotypes and for IgD in the Horse. J Immunol 173: 3230-3242.

15. Shade C, Kai-Ting C, Anthony RM (2013) Antibody Glycosylation and Inflammation. Antibodies 2: 392-414.

16. Radaev S, Sun PD (2001) Recognition of IgG by Fcgamma receptor. The role of Fc glycosylation and the binding of peptide inhibitors. J Biol Chem 276: 16478-16483.

17. Ha S, Ou Y, Vlasak J, Li Y, Wang S, et al. (2011) Isolation and characterization of IgG1 with asymmetrical Fc glycosylation. Glycobiology 21: 1087-1096.

18. Zauner G, Selman MH, Bondt A, Rombouts Y, Blank D, et al. Glycoproteomic analysis of antibodies. Mol Cell Proteomics 12: 856-865.

19. Hayes JM, Cosgrave EF, Struwe WB, Wormald M, Davey GP, et al. Glycosylation and Fc receptors. Curr Top Microbiol Immunol 382: 165-199.

20. Fernandes D (2005) Demonstrating Comparability of Antibody Glycosylation during Biomanufacturing. Eur Biopharma Rev: 106-110.

21. Winters-Hilt S, Morales E, Amin I, Stoyanov A (2007) Nanopore-based kinetics analysis of individual antibody-channel and antibody antigen interactions. BMC Bioinformatics 8: S7-S20.

22. Stephen Winters-Hilt, Wenonah Vercoutere,Veronica S DeGuzman, David Deamer, Mark Akeson, et al. (2003) Highly Accurate Classification of Watson-Crick Basepairs on Termini of Single DNA Molecules. Biophys J 84: 967-976.

23. Vercoutere W, S Winters-Hilt, H Olsen, D Deamer, D Haussler, M Akeson (2001) Rapid Discrimination Among Individual DNA Molecules at Single Nucleotide Resolution Using an Ion Channel. Nat Biotechnol 19: 248-252.

24. Xiang D, Shigdar S, Qiao G, Wang T, Kouzani AZ, et al. (2015) Nucleic Acid Aptamer-Guided Cancer Therapeutics and Diagnostics: the Next Generation of Cancer Medicine. Theranostics 5: 23-42.

25. Germer K, Leonard M, Zhang X (2013) RNA aptamers and their therapeutic and diagnostic applications. Int J Biochem Mol Biol 4: 27-40.

26. Ming X, Laing B (2015) Bioconjugates for targeted delivery of therapeutic oligonucleotides. Adv Drug Deliv Rev 87: 81-89.

27. Meyer C, Hahn U, Rentmeister A (2011) Cell-Specific Aptamers as Emerging Therapeutics. J. Nucl. Acids.

28. Lee JW, Kim HJ, Heo K (2015) Therapeutic aptamers: developmental potential as anticancer drugs. BMB Rep 48: 234-237.

29. Winters-Hilt S (2017) Finite State Automata with Bootstrap Learning.